

Surface superconductivity as the primary cause of broadening of superconducting transition in Nb-films

A. Zeinali and V. M. Krasnov*

¹*Department of Physics, Stockholm University, AlbaNova University Center, SE-10691 Stockholm, Sweden*

We study the origin of broadening of superconducting transition in sputtered Nb films. From simultaneous tunneling and transport measurements we conclude that the upper critical field H_{c2} always corresponds to the bottom of transition $R \sim 0$, while the top $R \sim R_n$ occurs close to the critical field for destruction of surface superconductivity $H_{c3} \simeq 1.7H_{c2}$. The two-dimensional nature of superconductivity at $H > H_{c2}$ is confirmed by cusp-like angular dependence of magnetoresistance. Our data indicates that surface superconductivity is remarkably robust even in disordered polycrystalline films and, surprisingly, even in perpendicular magnetic fields.

I. INTRODUCTION

Superconductivity occurs as a result of the second-order phase transition, accompanied by a sudden appearance of the superconducting order parameter below the critical temperature T_c and the upper critical field H_{c2} [1]. This should lead to an abrupt vanishing of resistance. However, in reality resistive transitions are always broadened, especially in magnetic field. This is usually ascribed to flux-flow phenomenon caused by motion of Abrikosov vortices [2]. Broadening can also be caused by spatial inhomogeneity (e.g. variation of T_c), or superconducting fluctuations [3–5], particularly for high temperature superconductors. Finally, surface superconductivity (SSC) may survive up to a significantly higher field $H_{c3} \simeq 1.69H_{c2}$ than bulk superconductivity [1], which can also smear the superconducting transition. Although SSC is quite profound in polished clean superconductors [6–9], it is usually ignored for disordered, polycrystalline films because SSC is considered to be very sensitive to the quality of the surface (e.g., surface passivation [8] and order parameter suppression [1]), surface roughness [6, 8] and surface scattering [10].

The broadening is detrimental for superconducting devices such as transition-edge sensors [11, 12] and resonators [8]. Presence of several mechanisms makes the interpretation of broadening ambiguous. The lack of understanding does not allow confident extraction of fundamental parameters of superconductors, such as H_{c2} , because it is unclear which point at the transition curve corresponds to $H = H_{c2}$. Arbitrary criteria, such as 10, 50 or 90 % of the normal state resistance R_n , are commonly applied which apparently does not work for high- T_c superconductors with very broad transitions [13]. Therefore, clarification of the mechanism of broadening is important both for fundamental and applied research on superconductors.

In this work we study the origin of broadening of superconducting transitions in sputtered Nb films. We perform simultaneous tunneling spectroscopy and transport mea-

surements, which allow unambiguous ascription of H_{c2} to the bottom of resistive transition $R(H_{c2})/R_n \sim 0$. The top of transition corresponds to ~ 1.7 times higher fields, which is close to the third critical field H_{c3} for destruction of surface superconductivity. The two-dimensional (2D) nature of SSC at $H_{c2} < H < H_{c3}$ is confirmed by observation of cusp-like angular dependence of magnetoresistance. Thus we conclude that surface superconductivity, rather than flux-flow, inhomogeneity or fluctuations, is the primary cause of broadening of superconducting transitions in magnetic field. Our data indicates that surface superconductivity is remarkably robust even in disordered polycrystalline films and, surprisingly, even in perpendicular magnetic fields.

II. EXPERIMENTAL

The studied sample contains several Nb/Al-AlO_x/Nb tunnel junctions with sputtered Nb electrodes of thicknesses $d = 150$ and 50 nm. Junction characteristics in perpendicular fields were reported in Ref. [14]. Due to different thicknesses, electrodes have slightly different T_c of 9.2 and 8.8 K. Parameters extracted from tunneling characteristics are determined by the thinner electrode, while transport measurements are made at the thicker electrode. This explains a minor difference in H_{c2} values obtained by those techniques. Measurements are performed in a gas-flow ⁴He cryostat with a superconducting solenoid. Samples are mounted on a rotatable holder with the alignment accuracy $\sim 0.02^\circ$. Details of the setup can be found elsewhere [14].

III. RESULTS

In Figures 1 (a-c) we show superconducting transitions of a 150 nm thick Nb film: (a) $R(T)$ in zero field and $R(H)$ at $T = 1.8$ K for field perpendicular (b) and parallel (c) to the film. It is seen that at zero field the $R(T)$ transition is very sharp and does not show any extended fluctuation region or inhomogeneity. However, $R(H)$ transitions are quite broad. Interestingly, $R(H)$ is broader when the field is parallel to the film. This

*Electronic address: Vladimir.Krasnov@fysik.su.se

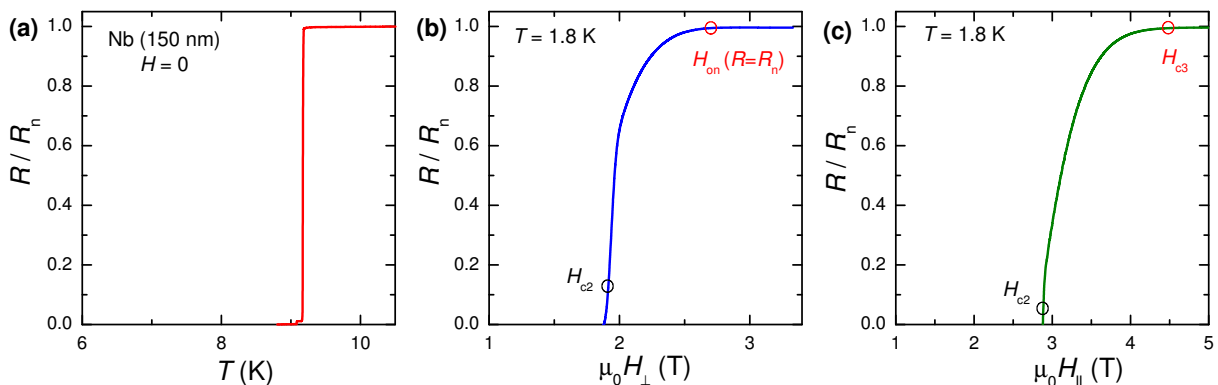


FIG. 1: (Color online). Resistive transitions of a 150 nm thick Nb film. (a) Temperature dependence of the resistance in zero magnetic field. (b) and (c) Field dependencies of resistances at $T = 1.8$ K in fields (b) perpendicular and (c) parallel to the film. Black and red circles mark the upper critical field H_{c2} and the field of the onset of resistive transition, which coincides with the critical field of surface superconductivity $H_{on} \sim H_{c3}$.

confronts interpretation of broadening in terms of vortex motion because the driving Lorentz force is most effective in perpendicular and vanishes in parallel field. Therefore, this broadening is not consistent with either flux-flow, inhomogeneity or fluctuation mechanisms.

A. Determination of H_{c2} from tunneling spectroscopy

In order to analyze surface superconductivity scenario, first of all, it is necessary to determine bulk H_{c2} . For this we perform magneto-tunneling spectroscopy. Figure 2 represents a comparison of theoretically calculated (a-c) and experimentally measured tunneling characteristics of our Nb/AlAlOx/Nb junction (data from Ref. [14]). Details of calculations are described in Ref. [14]). Panels (a) and (d) show temperature dependencies of I - V characteristics at zero field. Panels (b) and (e) show field dependence of I - V characteristics for field perpendicular to the junction/films at $T \simeq 2$ K. Panels (c) and (f) show the corresponding differential conductances for I - V curves from panels (b) and (e). There is a good quantitative agreement between theoretical and experimental characteristics. The main spectroscopic features are the sharp sum-gap peak at $V_p = 2\Delta/e$, where Δ is the superconducting gap and the suppressed quasiparticle current and conductance below the sum-gap voltage. With increasing field the peak is decreasing in height and is moving to lower voltages. Simultaneously the sub-gap conductance is increased. All this is due to suppression of the superconducting gap by magnetic field. The extent of suppression depends solely on H/H_{c2} . Above H_{c2} the superconducting gap vanishes and the I - V becomes linear (Ohmic). Thus, the ratio H/H_{c2} uniquely determines the shape of tunneling characteristics in magnetic field. Therefore, as discussed in Ref. [14], the ratio H/H_{c2} can be uniquely determined from analysis of the shape of tunneling characteristics. In Fig. 2 (f) the field is nor-

malized by thus obtained $H_{c2}^{\perp} = 1.61$ T. We emphasize that this value is obtained as a single fitting parameter for the whole set of $dI/dV(V)$ characteristics at different H . This removes the uncertainty in determination of H_{c2} .

Fig. 3 (a) shows a set of tunneling $dI/dV(V)$ characteristics of a Nb/AlOx/Nb junction at $T = 1.8$ K in fields parallel to Nb films. From comparison of Figs. 2 and 3 (a), it can be seen that the influence of magnetic field is qualitative similar both for parallel and perpendicular field orientations. In Ref. [14] it was shown that the peak height and the peak voltage exhibit universal almost T -independent quasi-linear scaling as a function of $H/H_{c2}(T)$. Fig. 3 (b) and (c) demonstrate such a scaling at different temperatures for field parallel to Nb films. Dashed and dashed-dotted lines in Fig. 3 (b) represent theoretical results from Ref. [14] for $T = 1.96$ and 4.7 K, correspondingly. The overall quality of scaling is quite good, which allows confident extraction of $H_{c2}(T)$. Thus obtained H_{c2} is unambiguous because it is deduced as a single fitting parameter for the whole set of $dI/dV(V)$ characteristics at fixed T for different H .

Squares in Figs. 3 (d) and (e) represent obtained $H_{c2}(T)$ dependencies for perpendicular and parallel field orientations, respectively. Using the relation $H_{c2}^{\perp} = \Phi_0/2\pi\xi^2$ we calculate the coherence length $\xi_0 \simeq 14$ nm. This small value indicates that the film is in the dirty limit with a very short scattering length due to a disordered film structure with nm-scale crystallites. Thus, the studied Nb film $d = 150$ nm is an order of magnitude thicker than ξ_0 . This leads to an important for a further discussion conclusion that our films are bulk three-dimensional (3D) superconductors practically in the whole temperature range $T < T_c$. Red circles in Figs. 1 (b) and (c) represent top onsets $R(H_{on}) \simeq R_n$ of resistive transitions. Dashed blue lines correspond to $H_{c3} = 1.69H_{c2}$ expected for surface superconductivity, which is close to the onset field. Remarkably this is true even for the perpendicular field orientation when SSC in

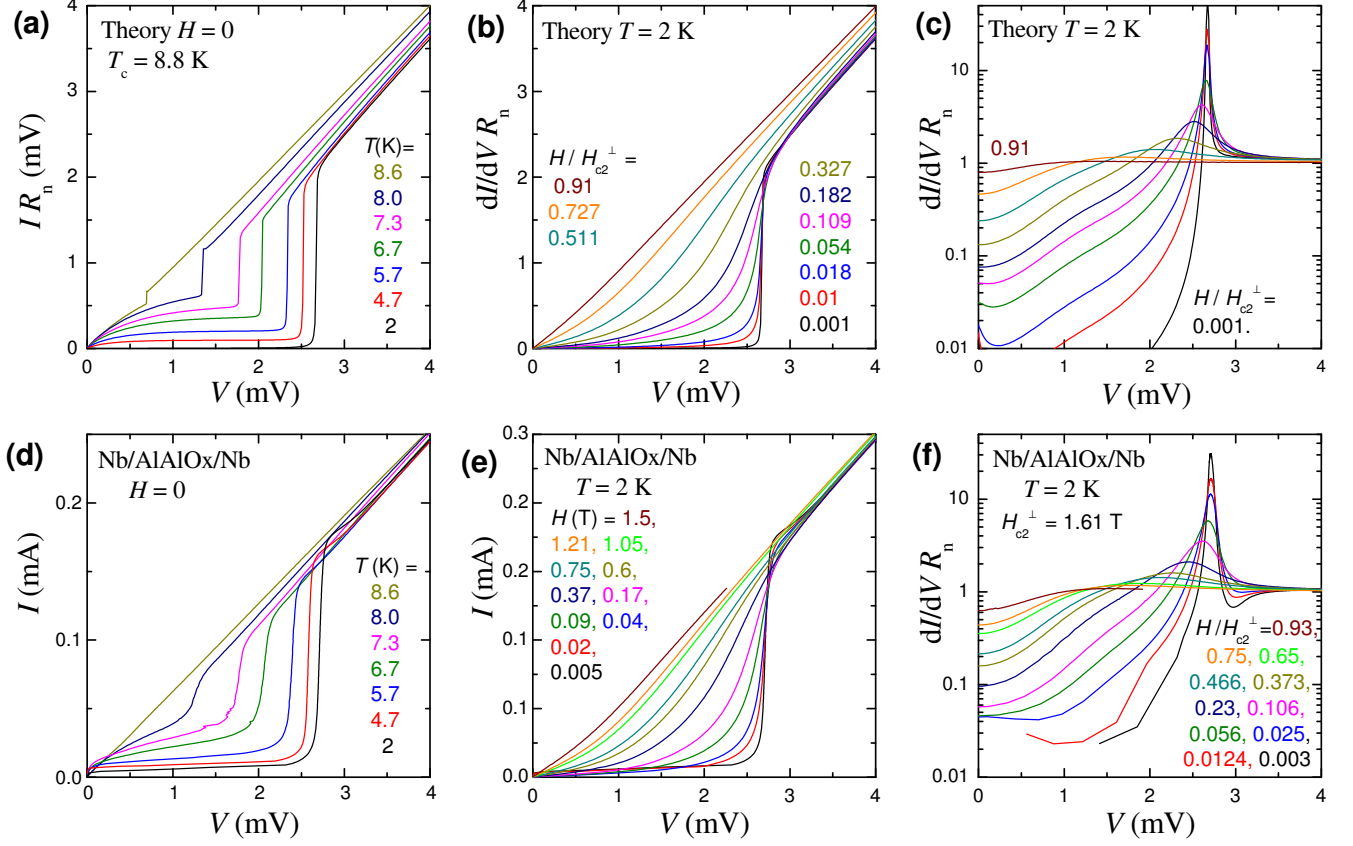


FIG. 2: (Color online). Comparison of theoretically calculated (a-c) and experimentally measured (d-f) characteristics of Nb/AlAlOx/Nb tunnel junctions. (a) and (d) Temperature dependence of I - V characteristics at zero field. (b) and (e) Field dependence of I - V characteristics for field perpendicular to the junction/films at $T \simeq 2$ K. (c) and (f) The corresponding differential conductances for curves from panels (b) and (e). The field scale in (f) is normalized by the upper critical field $H_{c2}^{\perp} = 1.61$ T, which is obtained as a single scaling factor for all the curves at different fields. Data from Ref. [14].

the uniform case is not expected [1].

B. Angular dependence of magnetoresistance

The 2D nature of SSC should be reflected in a cusp-like angular dependence of H_{c3} , given by the equation [15]:

$$\left[\frac{H_{c3}(\Theta)}{H_{c3}^{\parallel}} \cos \Theta \right]^2 A(\Theta) + \left| \frac{H_{c3}(\Theta)}{H_{c3}^{\perp}} \sin \Theta \right| = 1, \quad (1)$$

where $A(\Theta) = 1 + (1 - \sin \Theta) \tan \Theta$. It is only slightly different from Tinkham's 2D result with $A(\Theta) = 1$.

Fig. 3 (f) shows angular-dependencies of magnetoresistance at $T = 1.8$ K and at different fields below and above $\mu_0 H_{c2}^{\parallel} = 2.52$ T. Zero angle $\Theta = 0$ corresponds to field parallel to the film. It is seen that at 2.5 T very slightly below H_{c2} , $R(\Theta)$ is flat at $\Theta = 0$, which is characteristic for 3D bulk Nb. However, at $H > H_{c2}^{\parallel}$ angular dependence acquires a 2D cusp. Since the film thickness is much larger than ξ , the observed 2D behavior at low T may originate solely from SSC.

C. Non-linear bias dependence

The sheet surface critical current (in A/cm) is [16] :

$$I_c \simeq \frac{5}{2\sqrt{3}\pi} \frac{H_c}{\kappa} \left(1 - \frac{H}{H_{c3}} \right)^{3/2}. \quad (2)$$

Here H_c is the thermodynamic critical field (in Oe) and κ is the Ginzburg-Landau parameter. Typically such I_c is in the range from few to few tens of A/m. For our films with $\kappa \gg 1$ and the width of few microns the I_c is in the μ A range, comparable to the probe current. Therefore, the results do depend on the bias, as illustrated in Fig. 4 (a). This is due to strong non-linearity of current-voltage characteristics at $I \sim I_c$, as demonstrated in Fig. 4 (b). In order to demonstrate how such the non-linearity affects experimental characteristics we consider a standard shape of I - V :

$$V = R_n \sqrt{I^2 - I_c^2}. \quad (3)$$

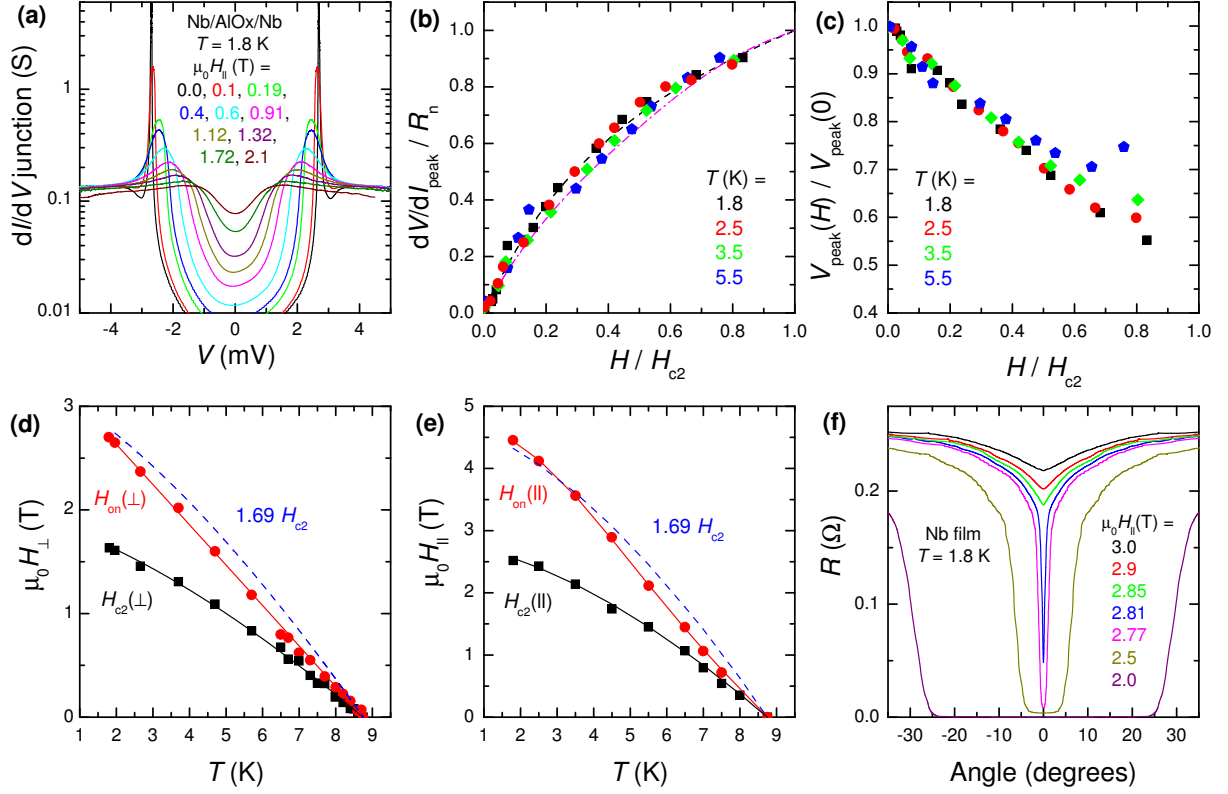


FIG. 3: (Color online). (a) Differential conductances of a Nb/AlOx/Nb junction (in a semi-logarithmic scale) at parallel to the films magnetic fields and $T = 1.8$ K. (b) and (c) Scaling of the sum-gap peak resistance (b) and voltage (c) as a function of $H/H_{c2}(T)$ at different temperatures and parallel fields. Dashed and dashed-dotted lines in (b) represent theoretical curves at $T = 1.96$ K and 4.7 K, respectively. (d) and (e) Black squares represent upper critical fields perpendicular (d) and parallel (e) to the films, obtained from the scaling of magneto-tunnelling characteristics. Dashed lines represent the expected third critical field for surface superconductivity $H_{c3} = 1.69H_{c2}$. Red circles mark the top onset of the resistive transition. (f) Angular dependence of resistance of Nb electrodes at fields slightly below and above $\mu_0 H_{c2}(\parallel) = 2.52$ T. A cusp-like feature at $H > H_{c2}$ indicates occurrence of the two-dimensional surface superconductivity.

Together with Eq. (2) it yields

$$1 - \left[\frac{R(\Theta)}{R_n} \right]^2 = \frac{I_c^2}{I^2} \left[1 - \frac{H}{H_{c3}(\Theta)} \right]^\nu. \quad (4)$$

The exponent ν depends on the shape of the I - V and the quality of the surface [6]. For the case of Eq. (3) it is $\nu = 3$.

In Fig. 4 (c) we show $R(\Theta)$ curves for the SSC model calculated from Eqs. (1) and (4) for $H = 1.1H_{c2}$ at different bias. Calculations are made for $H_{c3}^\perp = H_{c2}$ and $H_{c3}^\parallel = 1.69H_{c2}$ and for $I_c(\Theta) = \text{const}$. For comparison we also show flux-flow type dependence $R/R_n = H/H_{c3}$. It is seen that the cusp in the SSC model is much sharper, primarily due to non-linearity of the I - V . Overall behavior is similar to experimental data from Fig. 4 (a), even though in experiment a very sharp cusp at $\Theta = 0$ survives up to much higher current. The difference is due to an oversimplified assumption of angular-independent $I_c(\Theta) = \text{const}$, used in calculations. In reality $I_c(\Theta)$ has a sharp maximum at $\Theta = 0$ because the Lorentz force vanishes as $\sin(\Theta)$. It is possible to get a better fit us-

ing a more realistic $I_c(\Theta)$, but we don't want to go in to more complicated modelling because the main purpose of calculations was to demonstrate how non-linearity of I - V 's leads to a much sharper (compared to a simple 2D flux-flow model) cusp in $R(\Theta)$.

D. Analysis of fluctuation contribution

Finally we discuss fluctuation contribution to the broadening of resistive transition. In Fig. 5 (a) we show normalized excess conductance $\Delta S = (1/R - 1/R_n)R_n$ for the data from Figs. 1 (b) and (c) in a double-logarithmic scale. Such graph is usually used for analysis of fluctuation contribution to conductivity. Dashed line shows $\Delta S \propto (H - H_{c2})^{-1}$ dependence expected for 2D fluctuations [3]. It is seen that although there is a narrow range of fields close to H_{c2} with similar behavior, the overall agreement is poor. In Fig. 5 (b) we replot the same data in a semi-logarithmic scale. It is seen that ΔS decays quasi-exponentially with increasing field at

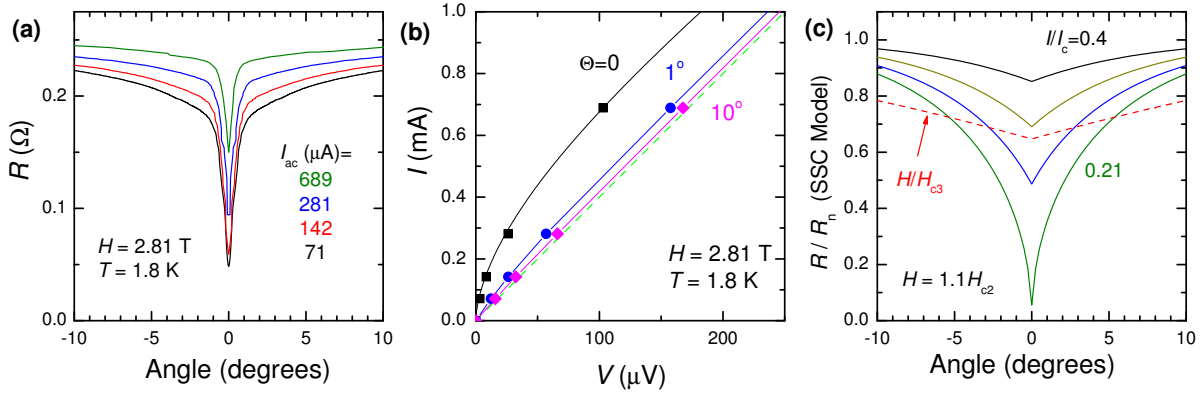


FIG. 4: (Color online). (a) Bias dependence of $R(\Theta)$ at $T = 1.8$ K and $H = 2.81$ T. (b) Deduced current-voltage characteristics at different angles from the data in panel (a). Dashed line represents the normal state I - V . (c) Simulated angular dependence of $R(\Theta)$ in the surface superconductivity model, taking into account non-linearity of I - V characteristics in the vicinity of critical current. Solid lines represent calculated of $R(\Theta)$ at different bias. Dashed curve represents the standard flux-flow dependence H/H_{c3} .

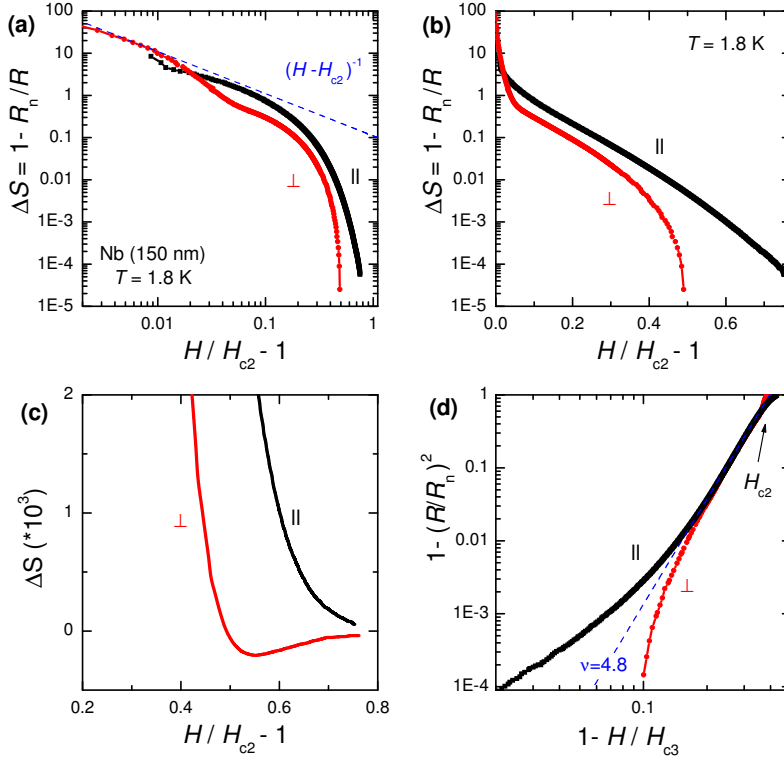


FIG. 5: (Color online). (a) and (b) Excess conductance vs. magnetic field at $T = 1.8$ K plotted in (a) a double-logarithmic and (b) a semi-logarithmic scale. Quasi-exponential decay $\Delta S(H)$ is seen. (c) The high-field part of excess conductance. It reveals fluctuation contribution, which is positive for parallel, but negative for perpendicular field orientation. (d) Analysis of power-law scaling expected for surface superconductivity according to Eq. (4). Dashed line represents a power-law with the exponent $\nu = 4.8$.

approximately the same rate for both field orientations. A similar exponentially decay versus both T and H has been reported for high- T_c cuprates [14, 17–19]. Here we demonstrate that it is generic also for conventional superconductors. Such behavior is not expected for fluctu-

ations [3–5] and we argue that it is rather a signature of SSC.

It is possible to distinguish fluctuation contribution from non-fluctuating SSC. SSC always leads to excess conductance, but fluctuation contribution to magnetore-

sistance can be both positive and negative [3–5]. In particular, at low T and at field perpendicular to the film the density-of-state contribution to fluctuations leads to excess resistance, rather than excess conductance [4]. We clearly see such a contribution in our data. In Fig. 5 (c) we show high-field part of excess conductance in the linear scale. It is seen that in parallel field there is always an excess conductance $\Delta S > 0$, which rapidly decreases upon approaching the surface critical field $H_{c3} \simeq 1.7H_{c2}^{\parallel}$, but never really vanishes. The remaining tail is a signature of fluctuations that persist at any field. For perpendicular field, ΔS at high fields becomes *negative*, which is consistent with theoretical expectations for fluctuation contribution at $T \ll T_c$ [4].

In Fig. 5 (d) we check the power-law scaling suggested by Eq. (4) for SSC. It is seen that there is a good scaling in a broad field range, although extraction of the exponent ν is not very confident because it depends on the choice of H_{c3} . The dashed line corresponds to $\nu = 4.8$. Upon approaching H_{c3} , deviations with opposite signs for parallel and perpendicular field orientations appear, signaling fluctuation contributions. This indicates that SSC makes a dominant contribution to excess conductivity at $H_{c2} < H \lesssim 0.8H_{c3}$, while fluctuation contribution starts to become significant only upon weakening of SSC at $H > 0.8H_{c3}$ and takes over completely at $H > H_{c3}$.

IV. DISCUSSION

Our results suggest that surface superconductivity is the primary cause of broadening of superconducting tran-

sition in magnetic field. As indicated in Figs. 1 (b) and (c), $H = H_{c2}$ corresponds to the bottom of transition, consistent with earlier studies [20], and H_{c3} to the top of the resistive transition. Thus the full width of the transition is dominated by SSC. Although SSC is well known for carefully polished single crystals [7, 9], it is usually considered to be insignificant for disordered, rough or inhomogeneous superconducting films because of its assumed fragility and sensitivity to surface conditions [1, 6, 8, 10]. Therefore, observation of a very robust SSC in our strongly disordered polycrystalline films is rather surprising, especially for field perpendicular to the film. In perfectly uniform films SSC should not occur at perpendicular field orientation [1, 16]. Yet, SSC in perpendicular fields has been directly visualized by scanning laser microscopy for similar films [21] and also reported for some layered superconductors [22] and sintered polycrystalline MgB₂ samples [23]. Presumably it is the polycrystallinity of our films that allows SSC at grain boundaries even in perpendicular fields. Thus we conclude that surface superconductivity is a robust phenomenon that should be carefully considered in analysis of data close to superconducting transition.

Acknowledgments

The work was supported by the Swedish Research Council Grant No. 621-2014-4314 and the Swedish Foundation for International Cooperation in Research and Higher Education Grant No. IG2013-5453.

-
- [1] D. Saint-James, G. Sarma, and E. J. Thomas, Type-II Superconductivity (Pergamon Press, Oxford, NY, 1969).
 - [2] J. Bardeen and M.J. Stephen, Theory of the Motion of Vortices in Superconductors, *Phys. Rev.* **140**, A1197 (1965).
 - [3] A.I. Larkin and A.A. Varlamov, Theory of Fluctuations in Superconductors, (Oxford University Press, New York, 2009).
 - [4] A. Glatz, A.A. Varlamov and V.M. Vinokur, Fluctuation spectroscopy of disordered two-dimensional superconductors, *Phys. Rev. B* **84**, 104510 (2011).
 - [5] K.S. Tikhonov, G. Schwiete, and A.M. Finkel'stein, Fluctuation conductivity in disordered superconducting films, *Phys. Rev. B* **85**, 174527 (2012).
 - [6] R. V. Bellau, Influence of surface condition on the critical currents above H_{c2} in a superconducting Tantalum-Niobium alloy, *Phys. Lett.* **21**, 13-16 (1966).
 - [7] S. R. Park, S.M. Choi, D. C. Dender, J.W. Lynn, and X. S. Ling, Fate of the Peak Effect in a Type-II Superconductor: Multicriticality in the Bragg-Glass Transition, *Phys. Rev. Lett.* **91**, 167003 (2003).
 - [8] S. Casalbuoni, E.A. Knabbe, J. Kötzer, L. Lilje, L. von Sawilski, P. Schmüser, B. Steffen, Surface superconductivity in niobium for superconducting RF cavities, *Nucl. Instr. & Methods in Phys. Res. A* **538**, 45-64 (2005).
 - [9] P. Das, C. V. Tomy, S. S. Banerjee, H. Takeya, S. Ramakrishnan, and A. K. Grover, Surface superconductivity, positive field cooled magnetization, and peak-effect phenomenon observed in a spherical single crystal of niobium, *Phys. Rev. B* **78**, 214504 (2008).
 - [10] D.F. Agterberg and M.B. Walker, Effect of diffusive boundaries on surface superconductivity in unconventional superconductors, *Phys. Rev. B* **53**, 15201 (1996).
 - [11] K. D. Irwin, G. C. Hilton, D. A. Wollman, and J.M. Martinis, X-ray detection using a superconducting transition-edge sensor microcalorimeter with electrothermal feedback, *Appl. Phys. Lett.* **69**, 1945 (1996).
 - [12] A. Lamas-Linares, B. Calkins, N. A. Tomlin, T. Gerrits, A.E. Lita, J. Beyer, R. P. Mirin, and S. W. Nam, Nanosecond-scale timing jitter for single photon detection in transition edge sensors, *Appl. Phys. Lett.* **102**, 231117 (2013).
 - [13] A. S. Alexandrov, V. N. Zavaritsky, W. Y. Liang, and P. L. Nevsky, Resistive Upper Critical Field of High- T_c Single Crystals of Bi₂Sr₂CaCu₂O₈, *Phys. Rev. Lett.* **76**, 983 (1996).
 - [14] V. M. Krasnov, H. Motzkau, T. Golod, A. Rydh, S. O. Katterwe and A. B. Kulakov, Comparative analysis of

- tunneling magnetoresistance in low- T_c Nb/Al-AlO_x/Nb and high- T_c Bi_{2-y}Pb_ySr₂CaCu₂O_{8+d} intrinsic Josephson junction, *Phys. Rev. B* **84**, 054516 (2011).
- [15] K. Yamafuji, E. Kusayanagi, and F. Irie, On the angular dependence of the surface superconducting critical field, *Phys. Lett.* **21**, 11-13 (1966).
- [16] A. A. Abrikosov, Concerning surface superconductivity in strong magnetic fields, *Sov. Phys. JETP* **20**, 480-488 (1965).
- [17] S. O. Katterwe, Th. Jacobs, A. Maljuk, and V. M. Krasnov, Low anisotropy of the upper critical field in a strongly anisotropic layered cuprate Bi_{2.15}Sr_{1.9}CuO_{6+δ}: Evidence for a paramagnetically limited superconductivity, *Phys. Rev. B* **89**, 214516 (2014).
- [18] F. Rullier-Albenque, H. Alloul, and G. Rikken, High-field studies of superconducting fluctuations in high- T_c cuprates: Evidence for a small gap distinct from the large pseudogap, *Phys. Rev. B* **84**, 014522 (2011).
- [19] H. Luo, and H.H. Wen, Localization of charge carriers in the normal state of underdoped Bi_{2+x}Sr_{2-x}CuO_{6+δ}, *Phys. Rev. B* **89**, 024506 (2014).
- [20] J. P. Burger, G. Deutscher, E. Guyon, and A. Martinet, Behavior of First- and Second-Kind Superconducting Films Near Their Critical Fields, *Phys. Rev.* **137**, A853 (1965).
- [21] R. Werner, A. Yu. Aladyshkin, I. M. Nefedov, A. V. Putilov, M. Kemmler, D. Bothner, A. Loerincz, K. Ilin, M. Siegel, R. Kleiner and D. Koelle, Edge superconductivity in Nb thin film microbridges revealed by electric transport measurements and visualized by scanning laser microscopy, *Supercond. Sci. Technol.* **26**, 095011 (2013).
- [22] F. Levy-Bertrand, B. Michon, J. Marcus, C. Marce-nat, J. Kačmarčík, T. Klein, and H. Cercellier, Puz-zling evidence for surface superconductivity in the lay-ered dichalcogenide Cu_{10%}TiSe₂, *Physica C* **523**, 19-22 (2016).
- [23] M. I. Tsindlekht, G.I. Leviev, V.M. Genkin, I. Felner, P. Mikheenko, and J.S. Abell, Surface superconducting states in a polycrystalline MgB₂ sample, *Phys. Rev. B* **74**, 132506 (2006).